# Immune Responses to COVID-19 mRNA Vaccines in Patients with Solid Tumors on Active, Immunosuppressive Cancer Therapy

Rachna T. Shroff[1,*], Pavani Chalasani[1,*], Ran Wei[2], Daniel Pennington[1], Grace Quirk[3], Marta V. Schoenle[2,3], Jennifer L. Uhrlaub[2], Tyler J. Ripperger[2], Mladen Jergović[2], Shelby Dalgai[1], Alexander Wolf, Hytham Hammad[1], Amy Carrier[1], Aaron J. Scott[1], Janko Nikolich-Žugich[2,3,6], Michael Worobey[3,4], Ryan Sprissler[3,5], Michael Dake[7], Bonnie J. LaFleur[3], and Deepta Bhattacharya[2,3]

*Both authors contributed equally to this work

[1] Division of Hematology and Oncology, Department of Medicine, University of Arizona Cancer Center, Tucson, AZ, USA.

[2]Department of Immunobiology, University of Arizona College of Medicine, Tucson, AZ, USA

[3] BIO5 Institute, University of Arizona, Tucson, AZ, USA

[4] Department of Ecology and Evolutionary Biology, University of Arizona, Tucson, AZ 85721, USA.

[5] University of Arizona Genomics Core and the Arizona Research Labs, University of Arizona Genetics Core, University of Arizona, Tucson, AZ, USA

[6] University of Arizona Center on Aging, University of Arizona College of Medicine, Tucson, AZ, USA

[7] Office of the Senior Vice-President for Health Sciences, University of Arizona, Tucson, AZ, USA

Corresponding authors: Rachna T. Shroff (rshroff@arizona.edu), Pavani Chalasani (pchalasani@uacc.arizona.edu), Bonnie LaFleur (blafleur@arizona.edu) and Deepta Bhattacharya (deeptab@arizona.edu).

**Abstract:**

Vaccines against SARS-CoV-2 have shown high efficacy, but immunocompromised participants were excluded from controlled clinical trials. We evaluated immune responses to the Pfizer/BioNTech mRNA vaccine in solid tumor patients (n=52) on active cytotoxic anti-cancer therapy. These responses were compared to a control cohort that also received the Pfizer/BioNTech vaccine (n=50). Using live SARS-CoV-2 assays, neutralizing antibodies were detected in 67% and 80% of cancer patients after the first and second immunizations, respectively, with a 3-fold increase in median titers after the booster. Similar trends were observed in serum antibodies against the receptor-binding domain (RBD) and S2 regions of Spike protein, and in IFN$\gamma$+ Spike-specific T cells. The magnitude of each of these responses was diminished relative to the control cohort. We therefore quantified RBD- and Spike S1-specific memory B cell subsets as predictors of anamnestic responses to viral exposures or additional immunizations. After the second vaccination, Spike-specific plasma cell-biased memory B cells were observed in most cancer patients at levels similar to those of the control cohort after the first immunization. These data suggest that a third immunization might elevate antibody responses in cancer patients to levels seen in healthy individuals after the second dose. Trials should be conducted to test these predictions.

**Main:**

The COVID-19 pandemic has led to over 150 million infections worldwide and claimed over 3 million lives to date. While non-pharmaceutical public health interventions managed to control outbreaks in certain countries, most of the global population will depend upon vaccines to mitigate the pandemic. Since the identification of SARS-CoV-2 as the causative agent of COVID-19 in January 2020[1,2], vaccines with very high efficacy have been developed and deployed with remarkable speed. Independent clinical trials demonstrated 94-95% vaccine efficacy against symptomatic disease caused by SARS-CoV-2 for both the Pfizer/BioNTech and Moderna mRNA-based vaccines[3,4]. Based on these data, in December 2020, both the Pfizer/BioNTech and Moderna vaccines were granted emergency use authorization by regulatory agencies in the United Kingdom and North America. Subsequent observational studies after authorization have shown that these vaccines also have high effectiveness against asymptomatic infections and suppress viral loads in breakthrough infections[5–8]. These data portend a marked overall reduction in community transmission once widespread vaccination is achieved.

These clinical trials, however, largely excluded immunocompromised individuals, including patients on immunosuppressive therapies to control chronic inflammatory conditions, primary immunodeficiencies, organ transplant recipients, and cancer patients on cytotoxic chemotherapy. As the number of deaths from this devastating virus has exceeded 575,000 in the US[9], concern about its impact on cancer patients has been high. This is especially true since a study from the COVID-19 Cancer Consortium

showed a 13% 30-day all-cause mortality from COVID-19 in a study of 928 patients[10]. Importantly, the investigators noted a higher risk of death in patients with active cancer.

Beyond the obvious direct benefits to these patients, vaccine-induced protection of immunocompromised individuals is of substantial indirect benefit to the general population. Some highly transmissible SARS-CoV-2 variants of concern that partially evade antibody responses are suspected to have arisen following prolonged evolution within immunocompromised patients[11–16]. Even partial vaccine-induced immunity is likely to reduce within-host viral population size and duration of within-host viral persistence and evolution, thereby slowing the emergence of future problematic variants[17]. Yet protective immune correlates of antibodies and memory B and T cells remain to be quantitatively defined[18]. Thus, optimal strategies are needed to elevate post-vaccination immunity in vulnerable immunocompromised populations to similar levels observed in healthy individuals. For individuals who cannot mount such an immune response, widespread community vaccination and targeted strategies to immunize close contacts will be required for indirect protection.

Several recent reports have shown diminished immune responses to SARS-CoV-2 infections and mRNA vaccines in subsets of immunocompromised patients, though these vary greatly with the nature of the immunosuppressive therapy. For example, patients with autoimmune conditions treated with B cell-depleting antibodies have predictably diminished humoral responses to vaccination, whereas responses by patients on anti-TNF$\alpha$ therapies are less affected[19]. As another example, organ transplant recipients mount very poor antibody responses to the first mRNA immunization relative to healthy individuals[20], but improve somewhat after the second

immunization[21]. Similarly, in cancer patients with solid or hematological malignancies, antibody responses are also markedly diminished after the first immunization but often improve after the second[22]. Yet because a relatively small group of these cancer patients was tested after the second immunization and because this group contained a mixture of those on cytotoxic chemotherapy and checkpoint blockade therapy, more data are required to instruct how best to protect this vulnerable population. It is possible that a third immunization may be beneficial.

We followed serological and cellular immune responses following mRNA vaccination of solid tumor patients on active cytotoxic chemotherapy. After the first immunization, we observed a higher fraction of patients with neutralizing antibodies than had previously been reported. Both the magnitude and frequency of these and T cell responses improved after the second vaccination but did not reach the levels observed in our control cohort. After the booster immunization, Spike RBD and other S1-specific memory B cells were observed in cancer patients at levels similar to those observed in healthy individuals after the first immunization. These data suggest that a third immunization may substantially benefit those who mount weak antibody responses.

**Results:**

Fifty-two patients with a known diagnosis of a solid tumor malignancy on active immunosuppressive cancer therapy were enrolled through the University of Arizona Cancer Center during their routine care. Participants in the control cohort were enrolled through the State of Arizona's COVID-19 vaccine point of distribution site at the University of Arizona during the phase 1B vaccination program. Eligible control cohort participants were enrolled while in the observational waiting area after their first vaccine shot (**Table 1**).

Blood samples for serological and cellular analyses were collected at the time of the first immunization, just prior to the second immunization, and again 5-9 days after the second vaccination (**Figure 1a**). Overall peripheral blood mononuclear cell (PBMC) counts were similar between the cancer and control cohorts (**Supplemental Figure 1a**). However, we noted a reduction in the frequency of CD19+ B cells and an increase in CD13+ myeloid cells in the cancer cohort relative to controls (**Supplemental Figures 1b-c**). Using serum from each of these samples, we first obtained single-dilution semi-quantitative data on Spike protein-specific antibody levels. For both the healthy and cancer cohort, we observed progressive increases after the first and second vaccinations in antibodies specific for the S2 region of Spike protein (**Figure 1b**). This region contains several antibody epitopes that are conserved across other common human □-coronaviruses[23–26], including at least one weakly neutralizing epitope[27,28]. Although both the cancer and control cohorts showed responses, median S2-specific antibody values were diminished in cancer patients relative to the control cohort at matched timepoints (**Figure 1b**). As most neutralizing and protective antibodies are

directed to the receptor binding domain (RBD) of Spike protein[29,30], we also semi-quantitatively determined the relative levels of these antibodies. Increases were also seen for RBD antibodies in both the healthy and cancer cohorts after each vaccination (**Figure 1c**). Yet as with antibodies against S2, the levels of RBD antibodies at draws 2 and 3 in the cancer cohort were diminished relative to healthy controls (**Figure 1c**). To obtain more quantitative information, we performed a full dilution series to determine antibody titers against RBD (**Supplemental Figure 1d**). Consistent with the semi-quantitative results, RBD antibody titers increased after the second immunization in both groups, but the median titers observed in the cancer cohort were reduced by >11-fold relative to healthy controls (**Figure 1d**).

For most vaccines, neutralizing antibody titers are the best correlate of protection from infections[31]. Early after vaccination, the total levels of RBD antibodies may not correlate especially well with neutralization, as many non-neutralizing specificities are generated[32]. We therefore directly assessed antibody-mediated neutralization of authentic live SARS-CoV-2 (WA1 isolate) after the first and second immunizations, as these assays tend to be more sensitive than those using pseudoviruses[33–36]. After the first shot, we observed a median plaque reduction neutralization test (PRNT)-90 titer of 60 in the control cohort and 20 in the cancer cohort (**Figure 2**). However, whereas all but one participant in the control cohort showed detectable virus neutralizing activity, this was observed in only 67% of the cancer cohort (**Figure 2**). After the second immunization, all healthy controls had virus-neutralizing antibodies, with a median PRNT90 titer of 540 (**Figure 2**). In contrast, 80% of the cancer cohort had detectable neutralizing antibodies with a median titer of 60 (**Figure 2**). These results demonstrated

that most of the cancer cohort generated protective antibodies, but at levels well below that of the control cohort after the second vaccine dose.

Prior studies have found that potentially protective T cell responses can be observed in COVID-19 convalescent individuals and in animal models when antibody levels are very low, such as after asymptomatic infections[37–40]. Moreover, the magnitude of T cell responses correlates relatively poorly with neutralizing antibody titers[41]. To quantify T cell responses in our healthy and cancer cohorts, peripheral blood mononuclear cells (PBMCs) were cultured overnight with either activating anti-CD3 antibodies (**Supplemental Figure 2**) or a pool of overlapping Spike protein peptides capable of presentation on both HLA-I and HLA-II (**Figure 3a**). ELISPOT assays were then performed to quantify interferon gamma (IFN$\gamma$)-producing T cells relative to paired control wells in which no peptides were added. In the control cohort, we observed a marked increase in the median frequency of IFN$\gamma$+ T cells after the first vaccination relative to pre-vaccination timepoints (2.9 fold, $p<0.0001$), and a further increase after the second vaccination (2.6 fold, $p<0.0001$, **Figure 3a**). Within the cancer cohort, the first vaccination did not induce a statistically significant increase in the median frequency of Spike-specific IFN$\gamma$+ T cells at draw 2, but a clear increase was observed at draw 3 (4-fold, $p<0.001$, **Figure 3a**). Accordingly, T cell frequencies were markedly reduced in the cancer cohort relative to healthy controls after the first vaccination, but approached the levels observed in the control cohort after the second vaccination (**Figure 3a**). The majority of these responses likely reflect Spike peptide-specific CD4+ T cells[42,43], though CD8+ T cells may also contribute[44–46]. Given the diminished T cell responses in the cancer cohort, more detailed analyses using either HLA-I or

HLA-II-restricted peptides and tetramers will be required to provide future insight on T cell subsets and responses.

To determine whether participants with poor neutralizing antibody titers might be partially protected by T cell responses, we examined T cell frequencies grouped by PRNT90 titers. Spike protein peptide-specific T cell frequencies at draw 1 were subtracted from the final draw 3 numbers to define individuals who mounted a response to vaccination. As has previously been described in post-infection responses[37,41], Spike protein peptide-specific T cell frequencies correlated relatively poorly with neutralizing antibody titers for both the healthy and cancer cohorts (**Figure 3b**). These data revealed that 4/10 cancer patients had detectable T cell responses even when PRNT90 titers were undetectable (**Figure 3b**). These data demonstrate that despite chemotherapy-induced immune suppression, relatively few cancer patients failed to make any detectable neutralizing antibody or T cell response.

Although most cancer patients mounted detectable antibody and T cell responses after vaccination, these levels in general did not reach those observed in the control cohort. The effectiveness of these diminished immune responses in preventing COVID-19 is difficult to predict. Recent studies have shown that the numbers of memory B cells are predictive of the magnitude of the response following booster vaccination[47]. Memory B cell subsets exhibit different behaviors in recall responses, generating either plasmablasts or new germinal centers[48–53]. These lineage potentials correlate with antibody isotype and other markers[48–53]. We therefore quantified RBD-specific memory B cell subsets after vaccination, including IgG+ and IgM+ CD27+ CD21+ classical resting memory B cells[53], CD27+ CD21- CD11c+ pre-plasmablast memory B cells[53–55],

and CD27- IgD- CD11c+ DN2 cells[54] (**Figure 4a, Supplemental Figure 3a**). We also measured memory B cells that bound the S1 region of spike protein but not RBD, as the N-terminal domain of S1 contains several neutralizing epitopes[56]. In the control cohort, we observed a clear increase in the frequency of isotype-switched RBD-binding CD21+ classical resting memory B cells as well as CD21- pre-plasmablast memory B cells after each vaccination (**Figure 4b**). Isotype-switched S1-binding CD21- memory B cells were also observed to increase after each vaccination of the control cohort (**Figure 4b**). Within the cancer cohort, we also observed isotype-switched RBD- and other S1-specific pre-plasmablast CD21- memory B cells, but only after the second immunization, and these levels were ~10-fold lower than those observed in the control cohort (**Figure 4b**). We were unable to detect isotype-switched RBD- or S1-specific classical resting memory B cells above pre-vaccination levels in the cancer cohort (**Figure 4b**). Some IgM+ and DN2 RBD- and S1-binding memory B cell subsets were detectable in the healthy and cancer cohorts, but in general the frequencies of these cells were substantially lower than the isotype-switched CD27+ subsets (**Supplemental Figure 3b**). Thus, RBD- and S1-specific cells early after vaccination are enriched in IgG+ memory subsets. These cells are biased towards plasma cell fates[51,53], though secondary germinal centers could conceivably arise from classical CD21+ memory cells[52].

We next examined whether RBD- and S1-specific memory B cells could be detected in cancer patients with no or low levels of neutralizing antibodies. Prior studies have shown that memory B cell numbers and specificities correlate only modestly with serum antibodies[57–61]. CD21- RBD- and S1-specific memory B cell frequencies at draw 3 were added to DN2 RBD+ memory B cell frequencies for each cancer patient, as these subsets were the only ones in which cancer patients consistently showed vaccine-induced increases (**Figure 4b** and **Supplemental Figure 3b**). Next, the corresponding pre-vaccination draw 1 frequencies were subtracted to correct for background levels in each patient. These net memory B cell frequencies were then plotted as a function of virus neutralization titers. Patients without detectable neutralizing antibodies also generally lacked RBD- and S1-specific memory B cells (**Figure 4c**). In contrast, patients with modest but detectable neutralizing antibody titers consistently showed RBD- and S1-specific memory B cells after the second immunization (**Figure 4c**). These data suggest that patients with low but detectable Spike-specific antibodies will likely generate anamnestic responses after a third immunization, conceivably approaching levels seen in healthy controls after the second vaccination. However, those who lack any detectable antibodies after two immunizations may be unlikely to generate such responses, irrespective of the number of additional booster immunizations.

**Discussion:**

The COVID-19 pandemic has dramatically affected the world, with a profound impact on cancer patients and their care. With high rates of transmission, even mitigation strategies have not been enough to decrease mortality rates from COVID-19 in patients with active cancer. Thus, the development of mRNA vaccines directed against SARS-CoV-2 was anxiously awaited in the cancer community. Given that the Pfizer/BioNTech trials did not include patients with active malignancies[3], the efficacy of these vaccines in solid tumor patients on active therapy was not reported. While prior studies in patients with colorectal and breast cancers on active chemotherapy who receive influenza vaccination show that patients can mount a serological response, the immunogenicity of the mRNA COVID vaccines in these patients is largely unknown[62,63]. A recent study in *JAMA* looked at 658 organ transplant recipients and demonstrated a lower antibody response after both doses of the mRNA COVID-19 vaccines when compared to immunocompetent participants[21]. Similarly, early studies suggest that cancer patients do not mount the same antibody responses as healthy controls[22].

Our results agree with certain aspects of these findings, but differ with and extend upon several key points. As with a recent study on immunocompromised cancer patients[22], we observed lower overall antibody and T cell responses compared with control cohorts. Yet in contrast to these findings, we observed that the majority of patients seroconverted after the first immunization, as measured by live virus neutralization assays. This frequency further increased after the second vaccination. These differences could potentially be explained by the nature of our cohort, which did not include patients on immunotherapy and as such may be more clinically

homogenous. In addition, neutralization assays using authentic viral isolates, as we used here, tend to be more sensitive than experiments performed with Spike protein-pseudotyped lentiviruses[33,34]. The ability to detect low levels of neutralizing antibodies is important when interpreting the potential value of vaccinating immunocompromised individuals.

There are several lines of evidence to suggest that the threshold for protection against COVID-19 may be relatively low. First, following natural infection, the levels of neutralizing antibodies are often quite low but symptomatic re-infections are rare[64–68]. Second, despite modest induction of overall immune responses, a single dose of mRNA vaccine provides reasonable protection against COVID-19[3–5]. Third, non-human primate studies have shown that low levels of passively transferred antibodies are protective against large infectious doses of SARS-CoV-2[40]. In these models, even when antibodies drop below protective levels, T cells can compensate and cooperate with residual antibodies to confer protection[40]. T cell responses are likely protective against severe disease in humans as well[37,38,69]. In this sense, it is encouraging that we also observed T cell responses in the majority of vaccinated cancer patients, including nearly half that mounted undetectable neutralizing antibody responses. Together, these data suggest that vaccination will confer at least partial protection and reduce the likelihood of severe COVID-19 in most cancer patients. The duration of this protection remains to be determined.

Nonetheless, when compared with individuals not on immunosuppressive therapy, the magnitudes of vaccine-induced antibody and T cell responses were substantially reduced in cancer patients, with several participants in our cohort failing to

mount any detectable antibody or T cell response. This seems likely to diminish vaccine effectiveness relative to the benchmark of 94-95% in non-immunocompromised populations[3,4]. Our cancer cohort naturally had an expected heterogeneity in terms of cancer diagnoses, the types of cytotoxic therapy patients received, and the timing of these therapies relative to vaccine dose. Thus, it is difficult to draw conclusions related to which solid tumors were associated with a better vaccine response or which therapies correlated with the non-responders. Yet it is worth noting that most of the non-responders had blood collected for immune analysis 7-14 days after their most recent treatment with cytotoxic agents. This time course is aligned with a nadir in blood counts and the peak of myelosuppression from traditional chemotherapy agents. While the numbers are too small to draw strong conclusions, these findings are certainly hypothesis-generating and merit further exploration to better understand the ideal timing for vaccination in patients on active immunosuppressive therapy. Our cancer cohort was also on average older than participants in the control cohort. There did appear to be an age-moderated effect within the control group on anti-RBD titers, which in turn could impact the magnitude of the differences we observed between the control and cancer cohorts. Yet no other immunological parameters were similarly affected and we did not observe age-moderated effects within the cancer cohort for any immunological parameter. Thus, the major driver of diminished responses in the cancer cohort is likely to be anti-cancer therapy rather than age.

One potential strategy to improve protective immune responses and potentially vaccine effectiveness is to provide a third immunization. Since anamnestic antibody production would be initiated by memory B cells, we measured antigen-specific subsets

after vaccination as a predictor of future recall responses[47]. Within the cancer cohort, we did not consistently detect unswitched IgM+ memory B cells thought to be capable of generating germinal center B cells[51], nor did we observe classical Spike-specific IgG memory cells. This may portend defects in the adaptation of antibody responses if exposed to problematic viral variants[60,70,71]. Yet we clearly observed RBD- and S1-specific CD21- memory B cells in most patients after the second vaccination. These subsets are plasma cell-biased and rapidly generate antibodies after immunization[53–55]. The frequencies of these memory B cells in the cancer cohort after the second vaccination were similar to those observed in our control cohort after the first immunization. Thus, our data would predict that after a third immunization, a large proportion of cancer patients would reach antibody levels similar to those of healthy individuals after their second vaccination and assumed to be protective. Given their vulnerability to COVID-19[10], trials should be conducted to test this possibility and to better understand the ideal timing of vaccination relative to cancer treatment thereby improving immune responses in cancer patients on active immunosuppressive therapy.

**Methods:**

*Participant Selection:* This protocol was approved by the University of Arizona Institutional Review Board and activated in January 2021. Participants were recruited to the control cohort during the Phase 1B Pima County COVID-19 vaccine rollout. Participants scheduled for vaccine appointments at Banner University Medical Center North site were approached with the IRB approved consent and sequentially enrolled. Thereafter, patients with cancer diagnosis were enrolled at the University of Arizona Cancer Center. Informed consent was obtained for all participants. Eligible solid tumor cancer patients had to have active disease and be receiving ongoing cytotoxic systemic therapy. Patients receiving immunotherapy were excluded. Demographic information was collected in addition to cancer diagnosis and type of anti-cancer therapy. Dates of last treatment prior to vaccine administration were also noted. In total, 73 control cohort participants were consented and 65 completed all three blood draws and both vaccine shots; five did not come in for their blood draw and eleven did not show up for their scheduled vaccinations. Fifty-six cancer patients were consented for the study and 52 completed all three blood draws and received both shots. All of the cancer cohort participants received the Pfizer Vaccine, 61 enrolled participants in the control cohort received the Pfizer vaccine and 12 received the Moderna vaccine. For consistency, analyses are restricted to those participants that received the Pfizer vaccine. There were four control cohort participants that were seropositive based on the University of Arizona COVID-19 ELISA pan-Ig Antibody Test; all of these participants were removed from analyses. The complete study sample size is 52 cancer cohort patients and 50 control cohort participants.

*Peripheral blood mononuclear cell and serum preparation:* Twenty mL of blood was collected by venipuncture in heparinized Vacutainer tubes (BD) and an additional 10 mL was collected in clot activating non-heparinized Vacutainer tubes. After >30 minutes at room temperature, non-heparinized tubes were spun at 1200 x g for 10 minutes, and serum was collected and frozen in 1 mL aliquots at -20°C. For peripheral blood mononuclear cells (PBMCs), 15 mL of Ficoll-Paque Plus (Fisher Scientific) was added to 50 ml Leucosep tubes (Greiner) and spun for 1 minute at 1000 x g to transfer the density gradient below the filter. Twenty mL of blood from the heparinized tubes were then poured into the top of the Leucosep tube and then spun at 1000 x g for 10 minutes at room temperature with the brake off. The top plasma layer was carefully collected and frozen at -20°C and the remaining supernatant containing PBMCs above the filter was poured into a new 50 mL conical tube containing 10 ml phosphate buffered saline (PBS) and spun at 250 x g for 10 minutes. Cell pellets were resuspended in RPMI media containing 10% fetal calf serum and counted on a ViCell XR (Beckman Coulter). Cells were resuspended to a concentration of 2 x $10^7$ cells/mL in RPMI media containing 10% fetal calf serum. An equal volume of 80% fetal calf serum + 20% dimethyl sulfoxide was added dropwise and inverted once to mix. Suspensions were distributed at 1 mL/cryovial and frozen overnight at -80°C in Mr. Frosty freezing chambers (Nalgene). Vials were then transferred to storage in liquid nitrogen.

*ELISAs and quantification of antibody titers:* Serological assays were performed as previously described[34]. RBD was purchased from GenScript (catalog # Z03483) and S2

subdomain of the SARS-CoV-2 S glycoprotein was purchased from Sino Biological (catalog # 40590-V08B). To obtain titers and single-dilution OD450 values, antigens were immobilized on high-adsorbency 384-well plates at 5 ng/ml. Plates were blocked with 1% non-fat dehydrated milk extract (Santa Cruz Biotechnology #sc-2325) in sterile PBS (Fisher Scientific Hyclone PBS #SH2035,) for 1 h, washed with PBS containing 0.05% Tween-20, and overlaid for 60 min with either a single 1:40 dilution or 5 serial 1:4 dilutions beginning at a 1:80 dilution of serum. Plates were then washed and incubated for 1hr in 1% PBS and milk containing anti-human Pan-Ig HRP conjugated antibody (Jackson ImmunoResearch catalog 109-035-064) at a concentration of 1:2000 for 1 h. Plates were washed with PBS-Tween solution followed by PBS wash. To develop, plates were incubated in tetramethylbenzidine prior to quenching with 2N $H_2SO_4$. Plates were read for 450nm absorbance on CLARIOstar Plus from BMG Labtech. All samples were also read at 630nm to detect any incomplete quenching. Any samples above background 630nm values were re-run. Area Under the Curve values were calculated in GraphPad Prism (v9).

*T cell assays:* Frozen PBMCs were thawed by mixing with 10 mL of pre-warmed RPMI 1640 media (Gibco) containing 10% fetal calf serum (Peak Serum #PS-FB1), 1X Penicillin-Streptomycin (HyClone #SV30010) and 0.03 mg/mL DNAse (Sigma #DN25-100) in a 15 mL conical tube and spun at 1650 rpm for 5 minutes. Cell pellets were resuspended in 1 mL of X-VIVO 15 media with Gentamicin and Phenol Red (VWR #12001-988) containing 5% male human AB serum (Sigma #H4522-100ML), and incubated in 24-well plates overnight at 37°C with 5% $CO_2$. 250 µL of each sample was

plated on a 96-well round bottom plate and spun at 1650 rpm for 3 minutes, and then resuspended in 150 µl X-VIVO 15 media with 5% male human AB serum containing either 0.6 nmol PepTivator SARS-CoV-2 Prot_S peptide pool (Miltenyi Biotec #130-126-701) for antigen specific T cell stimulation, or positive control anti-CD3 mAb CD3-2 from Human IFN-γ ELISpot plus kit (Mabtech #3420-4APT-2), or blank media as negative control. Cell suspensions were transferred to pre-coated IFN-γ ELISpot plates and incubated overnight at 37°C with 5% CO2. Plates were emptied, washed 5 times with 200 µl/well of PBS (Fisher Scientific Hyclone PBS #SH2035), and incubated for 2 hours at room temperature with 100 µl/well PBS containing 0.5% fetal calf serum and 1 µg/ml detection antibody (7-B6-1-biotin). Plates were washed as above and incubated for 1 hour at room temperature with 100 µl/well of PBS-0.5% FCS with 1:1000 diluted Streptavidin-ALP. Plates were washed as above and developed for 10-15 minutes with 100 µl/well substrate solution (BCIP/NBT-plus) until distinct spots emerged. Color development was stopped by washing extensively in tap water and left to dry. Spots were imaged and counted using an ImmunoSpot Versa (Cellular Technology Limited, Cleveland, OH) plate reader.

*Virus neutralization assays:* SARS Coronavirus 2, Isolate USA-WA1/2020 (BEI NR-52281) was passaged once on Vero (ATCC #CCL-81) cells at a multiplicity of infection of 0.01 for 48 hours. Supernatant and cell lysate were combined, subjected to a single freeze-thaw, and then centrifuged at 3000 rpm for 10 minutes to remove cell debris. Plaque reduction neutralization tests (PRNT) for SARS-CoV-2 were performed as previously described[34]. Briefly, Vero cells (ATCC # CCL-81) were plated in 96-well

tissue culture plates and grown overnight. Serial dilutions of serum samples were incubated with 100 plaque forming units of SARS-CoV-2 for 1 hour at 37°C. Plasma/serum dilutions plus virus were transferred to the cell plates and incubated for 2 hours at 37°C, 5% CO2 then overlaid with 1% methylcellulose. After 72 hours, plates were fixed with 10% Neutral Buffered Formalin for 30 minutes and stained with 1% crystal violet. Plaques were imaged using an ImmunoSpot Versa (Cellular Technology Limited, Cleveland, OH) plate reader. The most dilute serum concentration that led to 10 or fewer plaques was designated as the PRNT90 titer.

*Flow cytometry:* One mL of pre-warmed fetal calf serum was added to a frozen cryovial of PBMCs which was then rapidly thawed in a 37°C water bath. Samples were poured into 15 mL conical tubes containing 5 mL pre-warmed RPMI + 10% fetal calf serum and spun at 250 x g for 5 minutes, room temperature. Supernatants were removed and pellets were washed once with 500 ul PBS containing 5% adult bovine serum and 0.1% sodium azide (staining buffer). Cell pellets were then resuspended in 200 µl staining buffer containing 1µl each of anti-IgM-FITC (Biolegend clone MHM-88), anti-IgD-PerCP-Cy5.5 (Biolegend clone IA6-2), anti-CD11c-Alexa700 (Biolegend clone Bu15), anti-CD13-PE-Cy7 (Biolegend clone WM15), anti-CD19-APC-efluor-780 (eBioscience clone HIB19), anti-CD21-PE-Dazzle (Biolegend clone Bu32), anti-CD27-BV510 (Biolegend clone M-T271), anti-CD38-APC (Biolegend clone HIT2), RBD-PE tetramer, and S1-BV421 tetramer. Tetramer reagents were assembled by mixing 100µg/ml C-terminal Avitagged RBD or S1 (AcroBiosystems) with 100µg/ml streptavidin-PE (eBiosciences) or streptavidin-BV421 (Biolegend), respectively, at a 5:1

molar ratio in which 1/10 the final volume of streptavidin was added every 5 minutes. S1 and RBD tetramers were validated by staining 293T cells as a negative control or 293T-hACE2-expressing cells[72] (BEI Resources NR-52511) as a positive control. PBMC samples were stained for at least 20 minutes, washed, and filtered through 70 μm nylon mesh. Data were acquired on either a BD LSR2 or Fortessa flow cytometer. Data were analyzed using FlowJo software.

*Statistical methods:* The primary endpoint for this study was the change in antibody-mediated neutralization of authentic live SARS-CoV-2 PRNT90 titers from baseline to draw 3 between participants in the control cohort and cancer cohort. This primary endpoint, powered as a non-inferiority hypothesis, was whether vaccine-acquired PRNT90 titers were the same in immunocompromised patients compared to healthy individuals. These methods typically require estimating the outcome under a non-inferiority margin; however, this criterion is not necessary given the obvious superiority PRNT90 titers seen in healthy participants compared to cancer patients at draw 3. Therefore, all statistical tests are based on test statistics with two-sided hypotheses with Tukey adjusted significance levels set at 0.05. First, we tested the difference in means of final titers and response levels within blood draws and cohorts using two-sided, two-sample t-tests. Secondary analyses included comparing differences between pairwise differences in slope and between blood draws, e.g. draw 1 to draw 2 and draw 2 to draw 3 between cohorts using repeated measures analysis of variance (ANOVA) that adjusts for the correlation within an individual by use of an exchangeable covariance matrix and F-test statistics. Analysis of covariance was used

to evaluate whether age moderated the between cohorts draw 3 differences for the semi-quantitative 1:40 serum dilution ELISA for RBD and S2 spike proteins as well as RBD AUC and neutralizing Ab titers. All analyses were performed in GraphPad Prism 9 and the R programming language version 4.0.5.

**Acknowledgements:**

This work was supported by National Institutes of Health grants R01AI099108 and R01AI129945 (D.B.) and from University of Arizona funds. We thank Marion Pepper and Jason Netland (University of Washington) for technical assistance with tetramer stains.

**Competing interests:**

Sana Biotechnology has licensed intellectual property of D.B. and Washington University in St. Louis. D.B. is a co-founder of Clade Therapeutics. B.J.L. has a financial interest in Cofactor Genomics, Inc. and Iron Horse Dx. P.C. receives research funding from Pfizer, BioAtla, Zentalis, Genentech, Eli-Lilly, Phoenix Molecular Designs, Amgen, Radius Pharmaceuticals, Carrick Therapeutics, and Angiochem and served on advisory boards for Novartis, Eli Lilly, Zentalis, Astra-Zeneca, Amgen, Bayer, Asthenex, Prosigna, Heron, Puma Biotechnology and Oncosec. R.T.S. receives research funding from Merck, Rafael Pharmaceuticals, ImmunoVaccine, Bayer, SeaGen, Exelixis, Pieris, LOXO Oncology, Novocure, NuCana, QED and has served as a consultant/advisor to Merck, Servier, Astra-Zeneca, EMD Serono, Taiho, QED, Incyte, Genentech, Basilea.

**Data, Code, and Materials Availability:** Raw data and statistical analysis code are available upon request to the corresponding authors. Figures 1-4 have associated raw data. Data will be made available without restrictions unless linked to identifiers in patient health information. Unique biological materials, including patient sera and cells, are of limited quantity. When possible and upon reasonable request, we may be able to share extra materials in small quantities.

**References:**


1. Wu, F. *et al.* A new coronavirus associated with human respiratory disease in China. *Nature* **579**, 265–269 (2020).
2. Zhou, P. *et al.* A pneumonia outbreak associated with a new coronavirus of probable bat origin. *Nature* **579**, 270–273 (2020).
3. Polack, F. P. *et al.* Safety and Efficacy of the BNT162b2 mRNA Covid-19 Vaccine. *N. Engl. J. Med.* **0**, null (2020).
4. Baden, L. R. *et al.* Efficacy and Safety of the mRNA-1273 SARS-CoV-2 Vaccine. *N. Engl. J. Med.* **384**, 403–416 (2021).
5. Thompson, M. G. *et al.* Interim Estimates of Vaccine Effectiveness of BNT162b2 and mRNA-1273 COVID-19 Vaccines in Preventing SARS-CoV-2 Infection Among Health Care Personnel, First Responders, and Other Essential and Frontline Workers - Eight U.S. Locations, December 2020-March 2021. *MMWR Morb. Mortal. Wkly. Rep.* **70**, 495–500 (2021).
6. Abu-Raddad, L. J., Chemaitelly, H. & Butt, A. A. Effectiveness of the BNT162b2 Covid-19 Vaccine against the B.1.1.7 and B.1.351 Variants. *N. Engl. J. Med.* **0**, null (2021).
7. Dagan, N. *et al.* BNT162b2 mRNA Covid-19 Vaccine in a Nationwide Mass Vaccination Setting. *N. Engl. J. Med.* **384**, 1412–1423 (2021).
8. Levine-Tiefenbrun, M. *et al.* Initial report of decreased SARS-CoV-2 viral load after inoculation with the BNT162b2 vaccine. *Nat. Med.* 1–3 (2021) doi:10.1038/s41591-021-01316-7.
9. CDC. COVID Data Tracker. *Centers for Disease Control and Prevention*

https://covid.cdc.gov/covid-data-tracker (2020).

10. Kuderer, N. M. *et al.* Clinical impact of COVID-19 on patients with cancer (CCC19): a cohort study. *Lancet Lond. Engl.* **395**, 1907–1918 (2020).
11. Kemp, S. A. *et al.* SARS-CoV-2 evolution during treatment of chronic infection. *Nature* **592**, 277–282 (2021).
12. McCarthy, K. R. *et al.* Recurrent deletions in the SARS-CoV-2 spike glycoprotein drive antibody escape. *Science* **371**, 1139–1142 (2021).
13. Avanzato, V. A. *et al.* Case Study: Prolonged Infectious SARS-CoV-2 Shedding from an Asymptomatic Immunocompromised Individual with Cancer. *Cell* **183**, 1901-1912.e9 (2020).
14. Aydillo, T. *et al.* Shedding of Viable SARS-CoV-2 after Immunosuppressive Therapy for Cancer. *N. Engl. J. Med.* **383**, 2586–2588 (2020).
15. Choi, B. *et al.* Persistence and Evolution of SARS-CoV-2 in an Immunocompromised Host. *N. Engl. J. Med.* **383**, 2291–2293 (2020).
16. Hensley, M. K. *et al.* Intractable COVID-19 and Prolonged SARS-CoV-2 Replication in a CAR-T-cell Therapy Recipient: A Case Study. *Clin. Infect. Dis. Off. Publ. Infect. Dis. Soc. Am.* (2021) doi:10.1093/cid/ciab072.
17. Cobey, S., Larremore, D. B., Grad, Y. H. & Lipsitch, M. Concerns about SARS-CoV-2 evolution should not hold back efforts to expand vaccination. *Nat. Rev. Immunol.* **21**, 330–335 (2021).
18. Khoury, D. S. *et al.* What level of neutralising antibody protects from COVID-19? *medRxiv* 2021.03.09.21252641 (2021) doi:10.1101/2021.03.09.21252641.
19. Deepak, P. *et al.* Glucocorticoids and B Cell Depleting Agents Substantially Impair

Immunogenicity of mRNA Vaccines to SARS-CoV-2. *medRxiv* 2021.04.05.21254656 (2021) doi:10.1101/2021.04.05.21254656.

20. Boyarsky, B. J. *et al.* Immunogenicity of a Single Dose of SARS-CoV-2 Messenger RNA Vaccine in Solid Organ Transplant Recipients. *JAMA* **325**, 1784–1786 (2021).
21. Boyarsky, B. J. *et al.* Antibody Response to 2-Dose SARS-CoV-2 mRNA Vaccine Series in Solid Organ Transplant Recipients. *JAMA* (2021) doi:10.1001/jama.2021.7489.
22. Monin, L. *et al.* Safety and immunogenicity of one versus two doses of the COVID-19 vaccine BNT162b2 for patients with cancer: interim analysis of a prospective observational study. *Lancet Oncol.* S1470204521002138 (2021) doi:10.1016/S1470-2045(21)00213-8.
23. Ladner, J. T. *et al.* Epitope-resolved profiling of the SARS-CoV-2 antibody response identifies cross-reactivity with endemic human coronaviruses. *Cell Rep. Med.* **2**, 100189 (2021).
24. Anderson, E. M. *et al.* Seasonal human coronavirus antibodies are boosted upon SARS-CoV-2 infection but not associated with protection. *Cell* **184**, 1858-1864.e10 (2021).
25. Nguyen-Contant, P. *et al.* S Protein-Reactive IgG and Memory B Cell Production after Human SARS-CoV-2 Infection Includes Broad Reactivity to the S2 Subunit. *mBio* **11**, (2020).
26. Shrock, E. *et al.* Viral epitope profiling of COVID-19 patients reveals cross-reactivity and correlates of severity. *Science* **370**, (2020).
27. Ng, K. W. *et al.* Preexisting and de novo humoral immunity to SARS-CoV-2 in

humans. *Science* **370**, 1339–1343 (2020).

28. Song, G. *et al.* Cross-reactive serum and memory B cell responses to spike protein in SARS-CoV-2 and endemic coronavirus infection. *bioRxiv* 2020.09.22.308965 (2020) doi:10.1101/2020.09.22.308965.
29. Greaney, A. J. *et al.* The SARS-CoV-2 mRNA-1273 vaccine elicits more RBD-focused neutralization, but with broader antibody binding within the RBD. *bioRxiv* 2021.04.14.439844 (2021) doi:10.1101/2021.04.14.439844.
30. Piccoli, L. *et al.* Mapping Neutralizing and Immunodominant Sites on the SARS-CoV-2 Spike Receptor-Binding Domain by Structure-Guided High-Resolution Serology. *Cell* **183**, 1024-1042.e21 (2020).
31. Zinkernagel, R. M. & Hengartner, H. Protective ‘immunity’ by pre-existent neutralizing antibody titers and preactivated T cells but not by so-called ‘immunological memory’. *Immunol. Rev.* **211**, 310–319 (2006).
32. Amanat, F. *et al.* The plasmablast response to SARS-CoV-2 mRNA vaccination is dominated by non-neutralizing antibodies and targets both the NTD and the RBD. *medRxiv* 2021.03.07.21253098 (2021) doi:10.1101/2021.03.07.21253098.
33. Abayasingam, A. *et al.* Long-term persistence of RBD+ memory B cells encoding neutralizing antibodies in SARS-CoV-2 infection. *Cell Rep. Med.* **2**, 100228 (2021).
34. Ripperger, T. J. *et al.* Orthogonal SARS-CoV-2 Serological Assays Enable Surveillance of Low-Prevalence Communities and Reveal Durable Humoral Immunity. *Immunity* **53**, 925-933.e4 (2020).
35. Wec, A. Z. *et al.* Broad neutralization of SARS-related viruses by human monoclonal antibodies. *Science* **369**, 731–736 (2020).

36. Chi, X. *et al.* A neutralizing human antibody binds to the N-terminal domain of the Spike protein of SARS-CoV-2. *Science* (2020) doi:10.1126/science.abc6952.
37. Sekine, T. *et al.* Robust T Cell Immunity in Convalescent Individuals with Asymptomatic or Mild COVID-19. *Cell* **183**, 158-168.e14 (2020).
38. Rydyznski Moderbacher, C. *et al.* Antigen-Specific Adaptive Immunity to SARS-CoV-2 in Acute COVID-19 and Associations with Age and Disease Severity. *Cell* **183**, 996-1012.e19 (2020).
39. Ogbe, A. *et al.* T cell assays differentiate clinical and subclinical SARS-CoV-2 infections from cross-reactive antiviral responses. *Nat. Commun.* **12**, 2055 (2021).
40. McMahan, K. *et al.* Correlates of protection against SARS-CoV-2 in rhesus macaques. *Nature* **590**, 630–634 (2021).
41. Reynolds, C. J. *et al.* Discordant neutralizing antibody and T cell responses in asymptomatic and mild SARS-CoV-2 infection. *Sci. Immunol.* **5**, (2020).
42. Anderson, E. J. *et al.* Safety and Immunogenicity of SARS-CoV-2 mRNA-1273 Vaccine in Older Adults. *N. Engl. J. Med.* **383**, 2427–2438 (2020).
43. Rodda, L. B. *et al.* Functional SARS-CoV-2-Specific Immune Memory Persists after Mild COVID-19. *Cell* **184**, 169-183.e17 (2021).
44. Sahin, U. *et al.* COVID-19 vaccine BNT162b1 elicits human antibody and T H 1 T cell responses. *Nature* **586**, 594–599 (2020).
45. Agerer, B. *et al.* SARS-CoV-2 mutations in MHC-I-restricted epitopes evade CD8+ T cell responses. *Sci. Immunol.* **6**, (2021).
46. Dan, J. M. *et al.* Immunological memory to SARS-CoV-2 assessed for up to 8 months after infection. *Science* (2021) doi:10.1126/science.abf4063.

47. Goel, R. R. *et al.* Distinct antibody and memory B cell responses in SARS-CoV-2 naïve and recovered individuals following mRNA vaccination. *Sci. Immunol.* **6**, (2021).

48. Dogan, I. *et al.* Multiple layers of B cell memory with different effector functions. *Nat. Immunol.* **10**, 1292–1299 (2009).

49. Pape, K. A., Taylor, J. J., Maul, R. W., Gearhart, P. J. & Jenkins, M. K. Different B cell populations mediate early and late memory during an endogenous immune response. *Science* **331**, 1203–7 (2011).

50. Zuccarino-Catania, G. V. *et al.* CD80 and PD-L2 define functionally distinct memory B cell subsets that are independent of antibody isotype. *Nat. Immunol.* **15**, 631–637 (2014).

51. Seifert, M. *et al.* Functional capacities of human IgM memory B cells in early inflammatory responses and secondary germinal center reactions. *Proc. Natl. Acad. Sci.* **112**, E546–E555 (2015).

52. Turner, J. S. *et al.* Human germinal centres engage memory and naive B cells after influenza vaccination. *Nature* **586**, 127–132 (2020).

53. Lau, D. *et al.* Low CD21 expression defines a population of recent germinal center graduates primed for plasma cell differentiation. *Sci. Immunol.* **2**, eaai8153 (2017).

54. Jenks, S. A. *et al.* Distinct Effector B Cells Induced by Unregulated Toll-like Receptor 7 Contribute to Pathogenic Responses in Systemic Lupus Erythematosus. *Immunity* **49**, 725-739.e6 (2018).

55. Knox, J. J. *et al.* T-bet+ B cells are induced by human viral infections and dominate the HIV gp140 response. *JCI Insight* **2**,.

56. McCallum, M. *et al.* N-terminal domain antigenic mapping reveals a site of vulnerability for SARS-CoV-2. *Cell* **184**, 2332-2347.e16 (2021).

57. Amanna, I. J. Duration of Humoral Immunity to Common Viral and Vaccine Antigens. *N. Engl. J. Med.* **357**, 1903–1915 (2007).

58. Lavinder, J. J. *et al.* Identification and characterization of the constituent human serum antibodies elicited by vaccination. *Proc. Natl. Acad. Sci. U. S. A.* (2014) doi:10.1073/pnas.1317793111.

59. Purtha, W. E., Tedder, T. F., Johnson, S., Bhattacharya, D. & Diamond, M. S. Memory B cells, but not long-lived plasma cells, possess antigen specificities for viral escape mutants. *J. Exp. Med.* **208**, 2599–2606 (2011).

60. Wong, R. *et al.* Affinity-Restricted Memory B Cells Dominate Recall Responses to Heterologous Flaviviruses. *Immunity* **53**, 1078-1094.e7 (2020).

61. Smith, K. G. C., Light, A., Nossal, G. J. V. & Tarlinton, D. M. The extent of affinity maturation differs between the memory and antibody-forming cell compartments in the primary immune response. *EMBO J.* **16**, 2996–3006 (1997).

62. Wumkes, M. L. *et al.* Serum antibody response to influenza virus vaccination during chemotherapy treatment in adult patients with solid tumours. *Vaccine* **31**, 6177–6184 (2013).

63. Puthillath, A. *et al.* Serological immune responses to influenza vaccine in patients with colorectal cancer. *Cancer Chemother. Pharmacol.* **67**, 111–115 (2011).

64. Robbiani, D. F. *et al.* Convergent antibody responses to SARS-CoV-2 in convalescent individuals. *Nature* **584**, 437–442 (2020).

65. Lumley, S. F. *et al.* Antibody Status and Incidence of SARS-CoV-2 Infection in

Health Care Workers. *N. Engl. J. Med.* **384**, 533–540 (2021).

66. Abu-Raddad, L. J. *et al.* Assessment of the risk of SARS-CoV-2 reinfection in an intense re-exposure setting. *Clin. Infect. Dis. Off. Publ. Infect. Dis. Soc. Am.* (2020) doi:10.1093/cid/ciaa1846.
67. Abu-Raddad, L. J. *et al.* SARS-CoV-2 antibody-positivity protects against reinfection for at least seven months with 95% efficacy. *EClinicalMedicine* **35**, (2021).
68. Long, Q.-X. *et al.* Clinical and immunological assessment of asymptomatic SARS-CoV-2 infections. *Nat. Med.* **10.1038/s41591-020-0965–6**, (2020).
69. Liao, M. *et al.* Single-cell landscape of bronchoalveolar immune cells in patients with COVID-19. *Nat. Med.* **26**, 842–844 (2020).
70. Mesin, L. *et al.* Restricted Clonality and Limited Germinal Center Reentry Characterize Memory B Cell Reactivation by Boosting. *Cell* **180**, 92-106.e11 (2020).
71. Leach, S. *et al.* Requirement for memory B-cell activation in protection from heterologous influenza virus reinfection. *Int. Immunol.* **31**, 771–779 (2019).
72. Starr, T. N. *et al.* Prospective mapping of viral mutations that escape antibodies used to treat COVID-19. *Science* **371**, 850–854 (2021).

**Table 1: Participant information.**

| | Cancer Cohort (N=52) | Control Cohort (N=50) |
|---|---|---|
| **Age** | | |
| Mean (SD) | 63.3 (9.56) | 41.3 (17.1) |
| **Gender** | | |
| Female | 42.0 (80.8%) | 33.0 (66.0%) |
| Male | 10.0 (19.2%) | 17.0 (34.0%) |
| **Prednisone** | | |
| Yes | 1.00 (1.9%) | 0 (0%) |
| No | 51.0 (98.1%) | 50.0 (100%) |
| **Recent Surgery** | | |
| Yes | 2.00 (3.8%) | 0 (0%) |
| No | 50.0 (96.2%) | 50.0 (100%) |
| **Other Vaccines** | | |
| Yes | 0 (0%) | 0 (0%) |
| No | 52.0 (100%) | 50.0 (100%) |
| **Prior COVID Infection** | | |
| Yes | 3.00 (5.8%) | 1.00 (2.0%) |
| No | 49.0 (94.2%) | 49.0 (98.0%) |
| **Radiation** | | |
| Yes | 18.0 (34.6%) | |
| No | 33.0 (63.5%) | |
| Missing | 1.00 (1.9%) | |
| **Days Since Treatment Prior to Draw 1** | | |
| Mean (SD) | 16.3 (51.2) | |
| **Days Since Treatment Prior to Draw 2** | | |
| Mean (SD) | 8.02 (7.64) | |
| **Days Since Treatment Prior to Draw 3** | | |
| Mean (SD) | 15.8 (8.09) | |
| **Tumor Type** | | |
| Gastroesophageal cancer | 3 (5.8%) | |
| Pancreatic cancer | 11 (21.1%) | |
| Biliary cancer | 4 (7.6%) | |
| Colorectal cancer | 9 (17.3%) | |
| Breast cancer | 23 (44.2%) | |
| Sarcoma | 1 (1.9%) | |
| Ovarian cancer | 1 (1.9%) | |
| **Chemotherapy**[¥] | | |
| IV Cytotoxic | 43 (82.6%) | |
| Oral Cytotoxic | 14 (26.9%) | |
| Concurrent hormonal therapy | 9 (17.3%) | |

[¥]not mutually exclusive therefore don’t sum to 100%

Figure 1

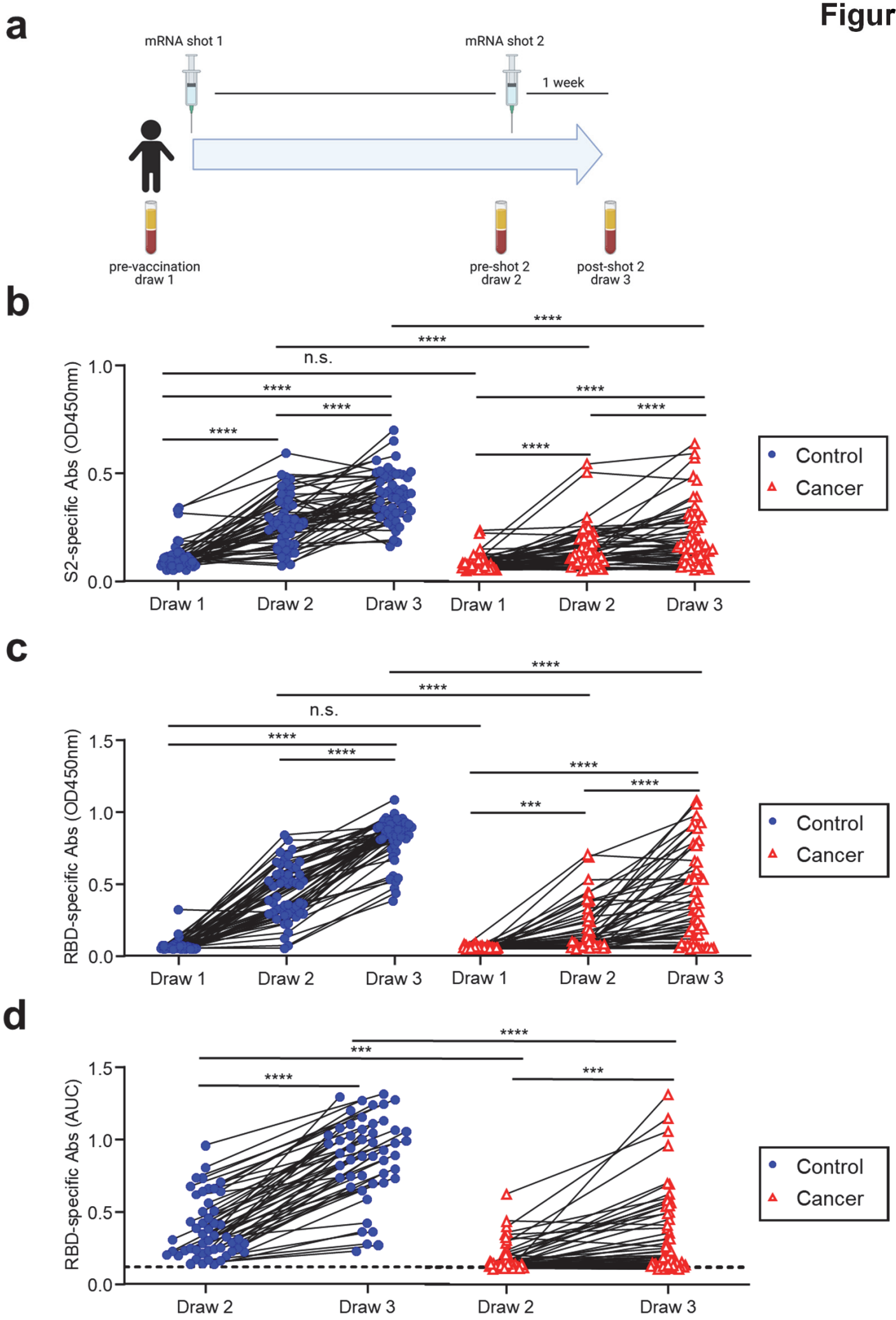
a
mRNA shot 1
mRNA shot 2
1 week
pre-vaccination draw 1
pre-shot 2 draw 2
post-shot 2 draw 3
b
S2-specific Abs (OD450nm)
1.0
0.5
0.0
n.s.
****
Draw 1
Draw 2
Draw 3
Control
Cancer
c
RBD-specific Abs (OD450nm)
1.5
1.0
0.5
0.0
n.s.
****
***
Draw 1
Draw 2
Draw 3
Control
Cancer
d
RBD-specific Abs (AUC)
1.5
1.0
0.5
0.0
****
***
Draw 2
Draw 3
Control
Cancer

**Figure 1: Antibody responses of cancer and control cohorts to mRNA vaccination. a,** Schematic of blood collection (draws) after vaccination. **b,** Semi-quantitative 1:40 serum dilution ELISA results for reactivity to the S2 region of SARS-CoV-2 Spike protein. Lines connect the same individual across timepoints. Repeated measures ANOVA examines the differences in slopes between cohorts, independently from the mean differences that were demonstrated at draw 3 between cohorts. There is a statistically significant difference in slopes between cancer and control cohorts ($p < 0.0001$) and the average rate of change is increasing at a steeper rate in the control cohort. These paired rates between draws by cohort are statistically different in the control compared to the cancer cohort for both draw 1 and draw 2, though it is not different between draw 2 and draw 3 (p-values $< 0.0001$ and 0.2945, respectively). **c,** Semi-quantitative 1:40 serum dilution ELISA results for reactivity to the receptor binding domain (RBD) of SARS-CoV-2 spike protein. Lines connect the same individual at each blood draw. There is a statistically significant difference in slopes between cancer and control cohorts ($p < 0.0001$) and the average rate of change is steeper in the control cohort. These paired rates between draws are statistically different in the control compared to the cancer cohort for both draw 1 and draw 2 and draw 2 and draw 3 (p-values $< 0.0001$ and 0.0043, respectively). **d,** Quantitative titers of RBD antibodies in control and cancer cohorts. A serum concentration beginning at 1:80 was serially diluted 1:4 and area under the curve (AUC) values calculated. Lines connect the same individual across timepoints. There is a statistically significant difference between draw 2 and draw 3 between cancer and control cohorts ($p < 0.0001$)

and the average rate of change is at a steeper increase in the control cohort.

***$p<0.001$; ****$p<0.0001$ by repeated measures ANOVA.

**Figure 2**

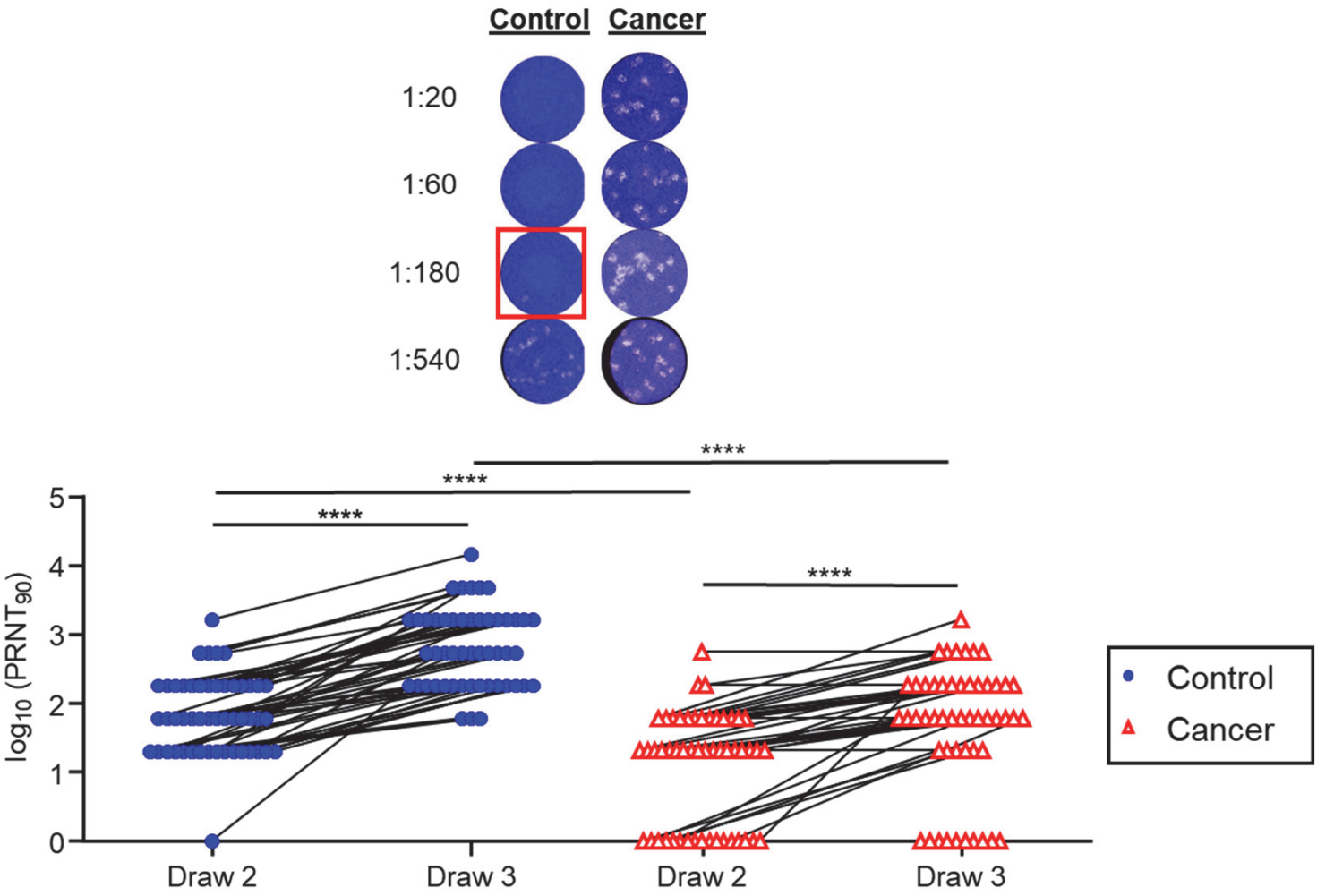
Control
Cancer
1:20
1:60
1:180
1:540
****
****
****
****
5
4
3
2
1
0
log10 (PRNT90)
Draw 2
Draw 3
Draw 2
Draw 3
Control
Cancer

**Figure 2: Neutralizing antibody responses of cancer and control cohorts to mRNA vaccination.** Virus neutralization assays were performed using the WA1 isolate of SARS-CoV-2. Serial 1:3 dilutions of serum were performed and tested for the ability to prevent plaques on Vero cells. The lowest concentration capable of preventing >90% of plaques was considered to be the PRNT90 value. Example images are shown for the control and cancer cohorts with the red box indicating the PRNT90 titer. Quantification is shown below. Lines connect the same individual across timepoints. There is a statistically significant difference between draw 2 and draw 3 between cancer and control cohorts ($p < 0.0001$) and the average rate of change is increasing at a steeper rate in the control cohort ($p = 0.0002$). ****$p<0.0001$ by repeated measures ANOVA.

Figure 3

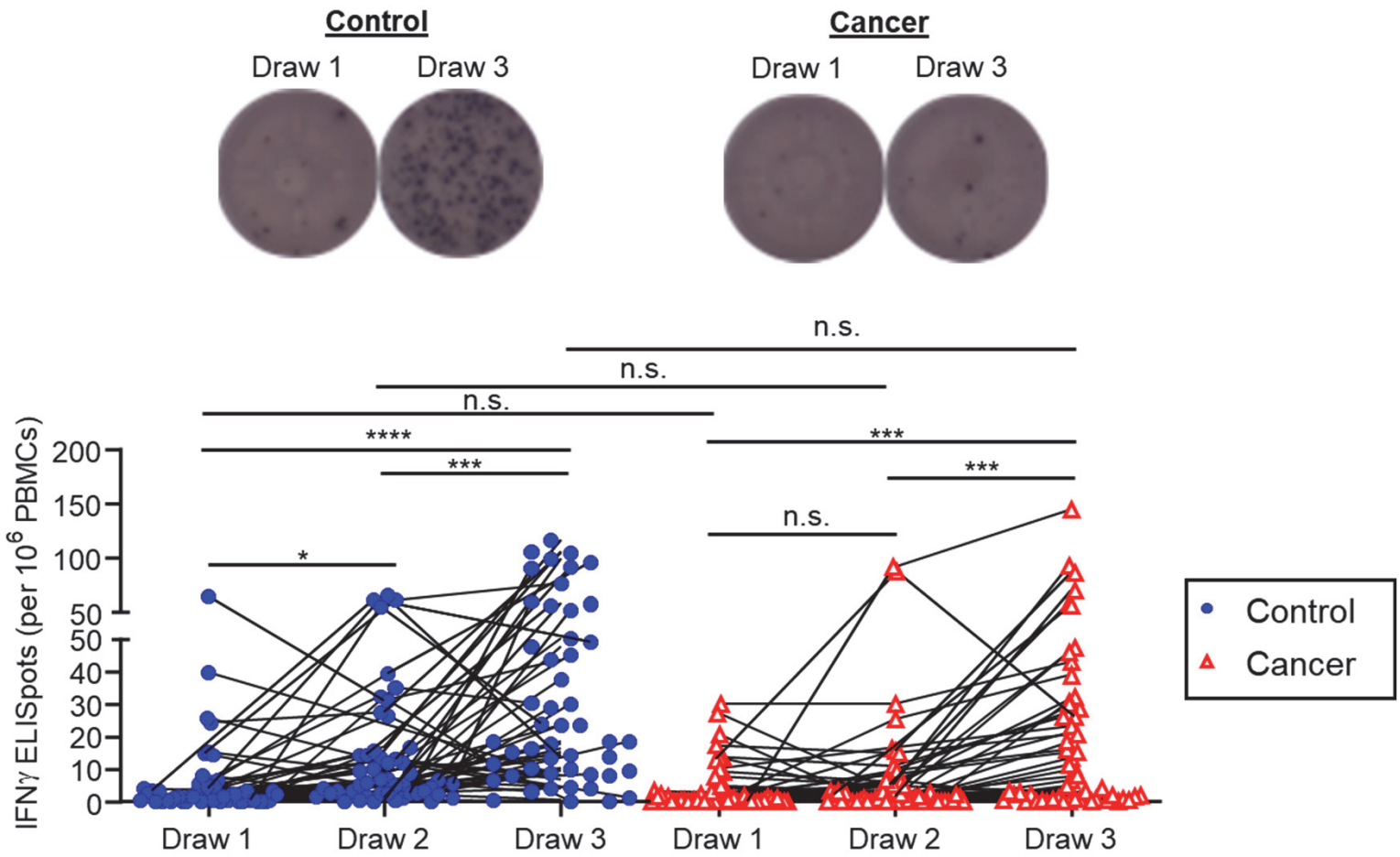
a
Control
Draw 1
Draw 3
Cancer
Draw 1
Draw 3
n.s.
n.s.
n.s.
****
***
***
***
n.s.
*
IFNγ ELISpots (per 10^6 PBMCs)
200
150
100
50
50
40
30
20
10
0
Draw 1
Draw 2
Draw 3
Draw 1
Draw 2
Draw 3
Control
Cancer

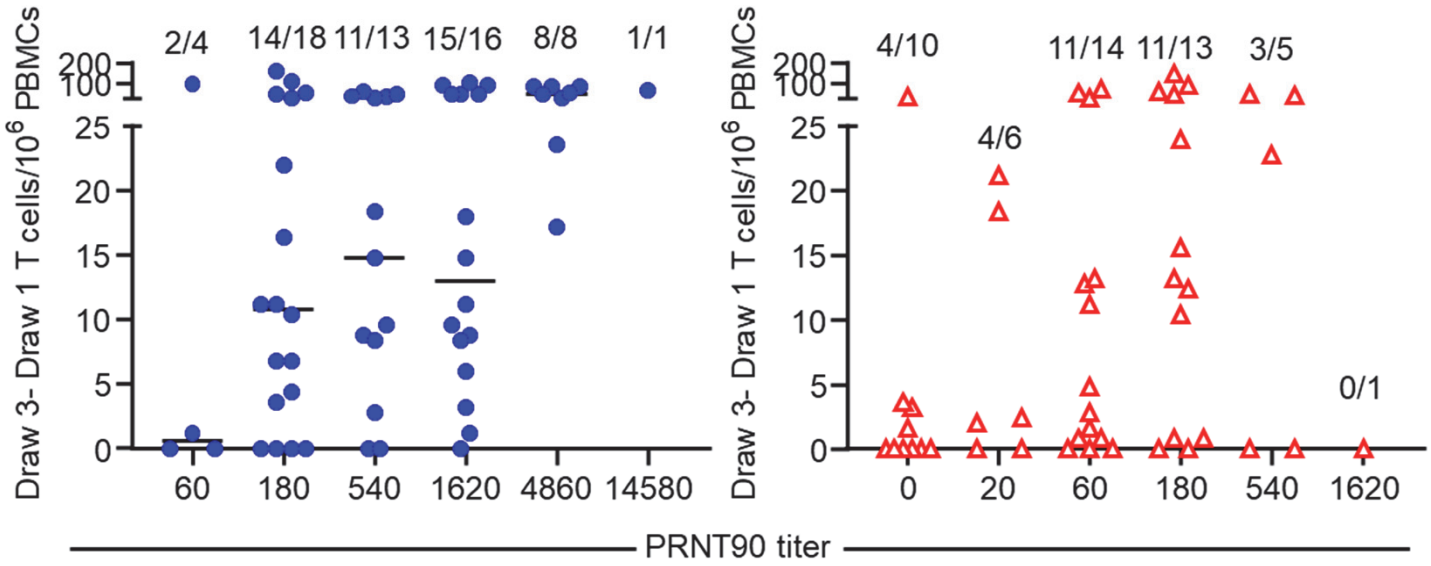
b
Draw 3- Draw 1 T cells/10^6 PBMCs
2/4
14/18
11/13
15/16
8/8
1/1
200
100
25
20
15
10
5
0
60
180
540
1620
4860
14580
Draw 3- Draw 1 T cells/10^6 PBMCs
4/10
4/6
11/14
11/13
3/5
0/1
0
20
60
180
540
1620
PRNT90 titer

**Figure 3: Spike-specific T cell responses of cancer and control cohorts to mRNA vaccination. a,** PBMCs were cultured for 24 h in the presence or absence of a pool of overlapping Spike protein peptides. IFN$\gamma$-producing cells were quantified by ELISPOT. Example images are shown for the control and cancer cohorts at timepoints 1 and 3. Quantification is shown below of the no peptide background-subtracted data. Lines connect the same individual across timepoints. There is a statistically significant difference in slopes between cancer and control cohorts ($p = 0.0284$) and the average rate of change is increasing steeper in the control cohort. While overall (draw 1 to draw 3, $p = 0.0455$) the rates of change between draw 1 to draw 2 and draw 2 to draw 3 were not statistically significant (p-values = 0.0642 and 0.9891, respectively). The inability to detect a statistical difference, particularly between draw 1 and draw 2, is likely due to sample size and variability as the cancer cohort difference is flatter than the cancer cohort between these two draws. **b,** Draw 1 Spike-specific T cell frequencies were subtracted from draw 3 frequencies as calculated in **a** and plotted by PRNT90 titers. Frequencies of individuals with detectable Spike-specific T cells are shown above each group; analyses were done on the log-transformed scale. There was a statistically significant difference in slopes between the cancer and control cohorts ($p = 0.0284$). The primary difference in rates between the two cohorts were between draw 1 and draw 3 ($p = 0.0455$), the differences between draw 1 and draw 2 and draw 2 and draw 3 were not statistically significantly different ($p = 0.0642$ and 0.9891, respectively). *$p<0.05$; ***$p<0.001$ by repeated measures ANOVA.

# Figure 4

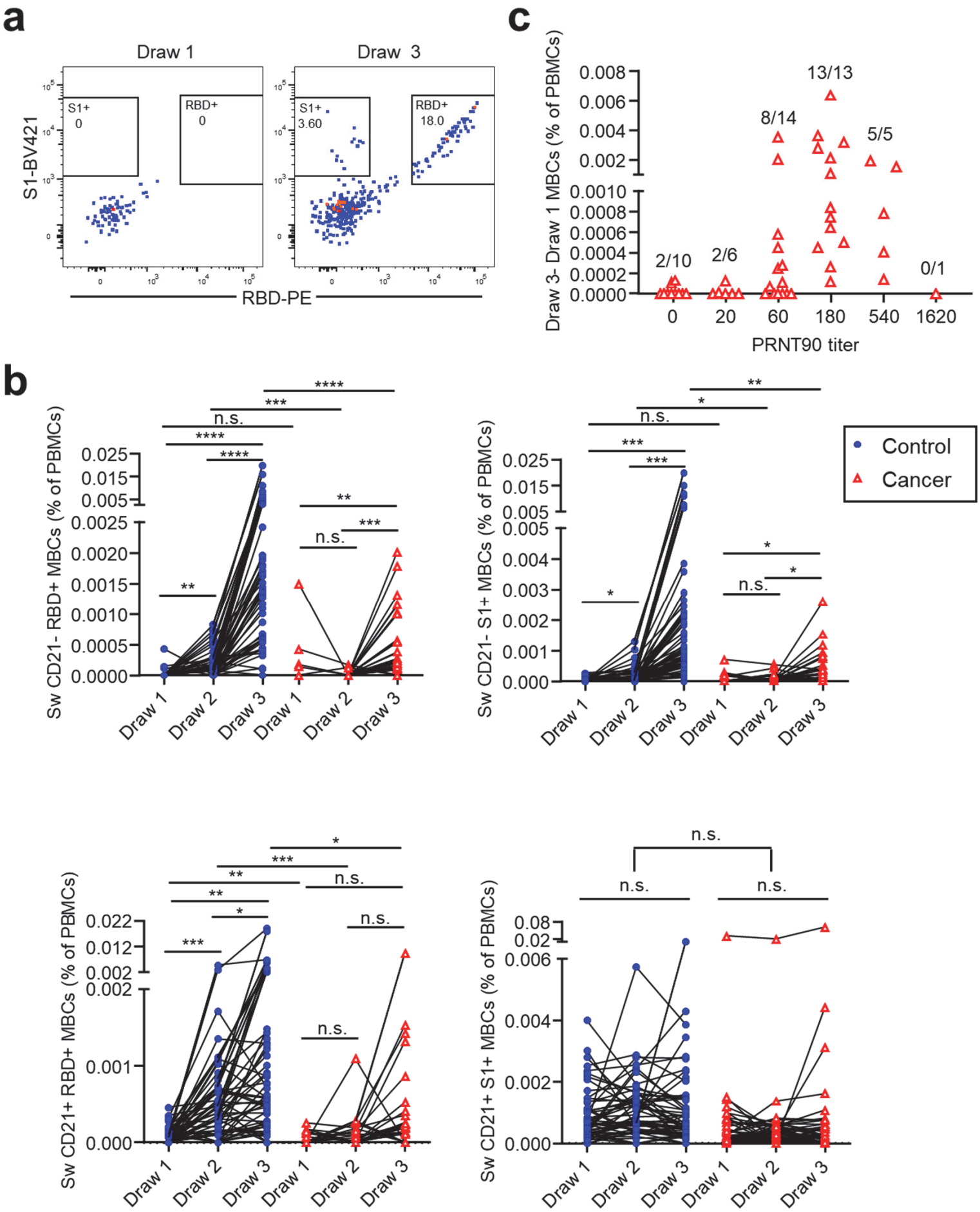
a
Draw 1
Draw 3
S1+
0
RBD+
0
S1+
3.60
RBD+
18.0
S1-BV421
RBD-PE
c
Draw 3- Draw 1 MBCs (% of PBMCs)
0.008
0.006
0.004
0.002
0.0010
0.0008
0.0006
0.0004
0.0002
0.0000
2/10
2/6
8/14
13/13
5/5
0/1
0
20
60
180
540
1620
PRNT90 titer
b
Sw CD21- RBD+ MBCs (% of PBMCs)
Sw CD21- S1+ MBCs (% of PBMCs)
Sw CD21+ RBD+ MBCs (% of PBMCs)
Sw CD21+ S1+ MBCs (% of PBMCs)
Draw 1
Draw 2
Draw 3
Control
Cancer
n.s.

**Figure 4: Memory B cell responses of cancer and control cohorts to mRNA vaccination. a,** Example gating strategy of RBD- and S1-specific CD21- isotype-switched memory B cells (full gating strategy is shown in **Supplemental Figure 3a**). **b,** Quantification of memory B cell subsets after vaccination. Isotype-switched (Sw) memory B cells expressing or lacking CD21 are shown in plots. Cells that bind both RBD and S1 are annotated as RBD+, whereas cells that are specific only for S1 are denoted as S1+. Lines connect the same individual across blood draws, analyses were done on the arcsin of the square-root transformation, to standardize the small percentages. There is a statistically significant difference in slopes between cancer and control cohorts for RBD+ and S1+ ($p < 0.0001$ and $< 0.0001$, respectfully) and the average rate of change is increasing in the control cohort for both RBD+ and S1+, though the magnitude is only statistically significant between draw 2 and 3 for RBD+ between the cancer cohort and the control cohort ($p=0.0991$ and $p< 0.0001$, respectively) and S1+ ($p = 0.3074$ and $< 0.0001$, respectively) . **c,** RBD-specific DN2 and S1- and RBD-specific isotype-switched CD21- memory B cells were added for the cancer cohort. Summed draw 1 memory B cell frequencies were subtracted from the summation of draw 3 frequencies for each individual . These values were grouped by PRNT90 titers. The average rate of change was statistically significantly different for RBD+ ($p < 0.0001$), with an increasing trend in the control cohort, and difference in rates between draw 1 and draw 2, and not between draw 2 and draw 3 ($p = 0.0160$ and 0.1059, respectfully). There was no statistically significant difference in slopes between cancer and control cohorts for S1+ ($p=0.2239$). Frequencies of individuals with

detectable memory B cells are shown above each group. *$p<0.05$; **$p<0.01$; ***$p<0.001$; ****$p<0.0001$ by repeated measures ANOVA.

# Supplemental Figure 1

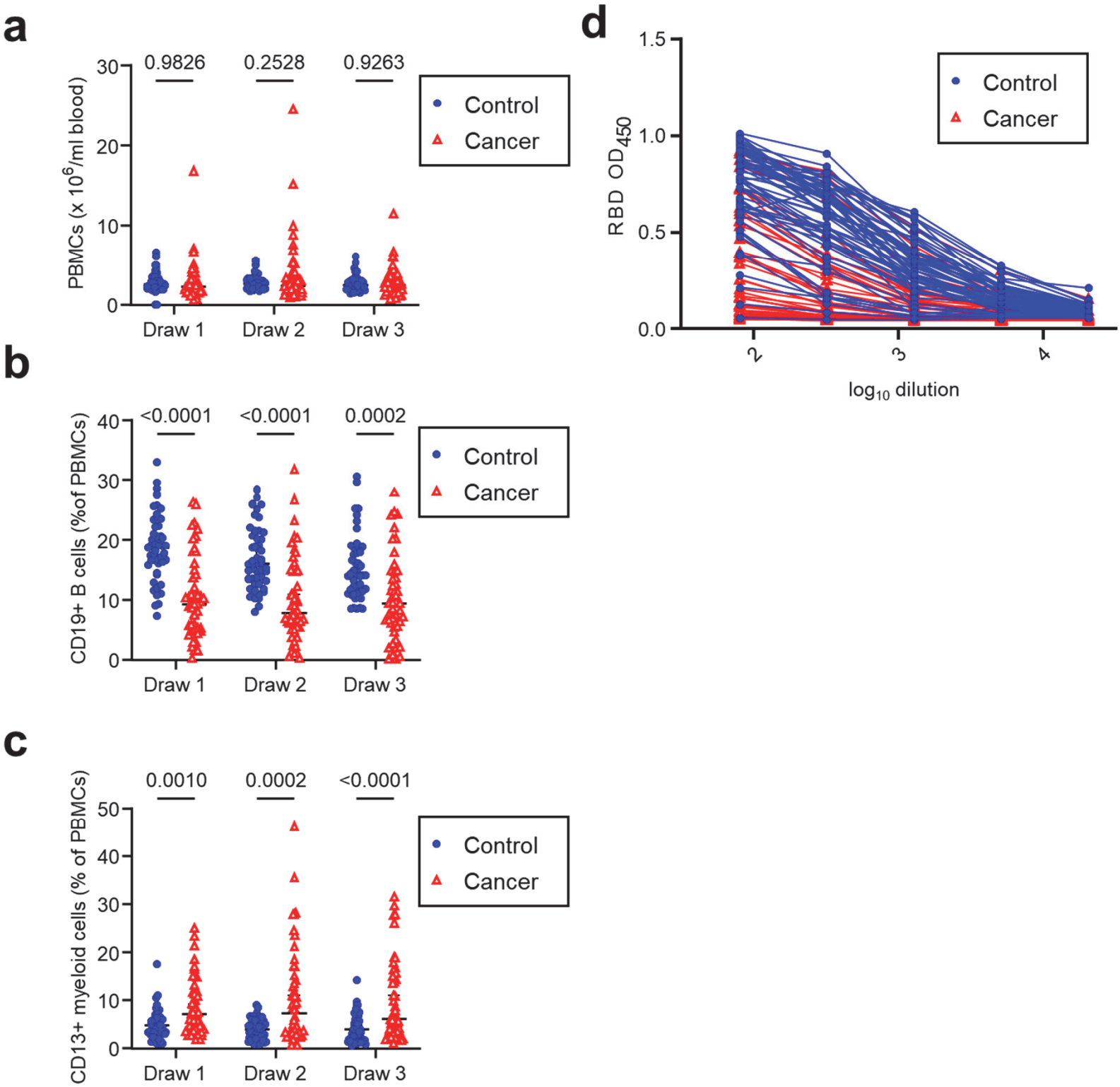

**Supplemental Figure 1: Cellular and serological characterization of blood samples from control and cancer cohorts. a,** PBMC frequencies of blood samples at each timepoint. P-values were calculated by 2-way ANOVA in which individual samples across blood draws were paired. **b,** CD19+ B cell frequencies of blood samples at each timepoint. P-values were calculated by 2-way ANOVA in which individual samples across blood draws were paired. **c,** CD13+ myeloid cell frequencies of blood samples at each blood draw. P-values were calculated by 2-way ANOVA in which individual samples across draws were paired. **d,** Raw ELISA data for quantification of RBD titers shown in **Figure 1d**. A serum concentration beginning at 1:80 was serially diluted and area under the curve (AUC) values calculated. Lines connect the same individual at each dilution. Data from the third blood draw are shown for both the control and cancer cohort. *$p<0.05$; **$p<0.01$; ***$p<0.001$; ****$p<0.0001$ by 2-way ANOVA.

# Supplemental Figure 2

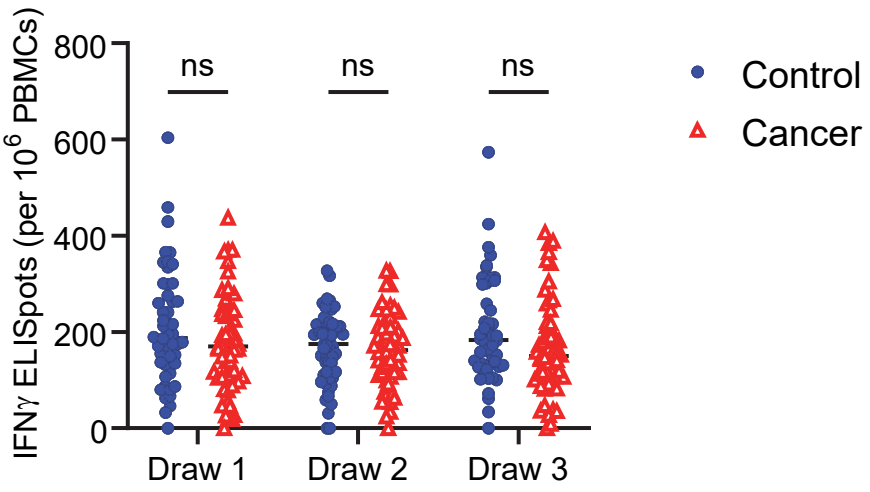

**Supplemental Figure 2: T cell activation in control and cancer cohorts.** PBMCs were cultured for 24 h in the presence of an activating anti-CD3 antibody. IFN$\gamma$-producing cells were quantified by ELISPOT. P-values were calculated by 2-way ANOVA in which individual samples across blood draws were paired.

# Supplemental Figure 3

**a**

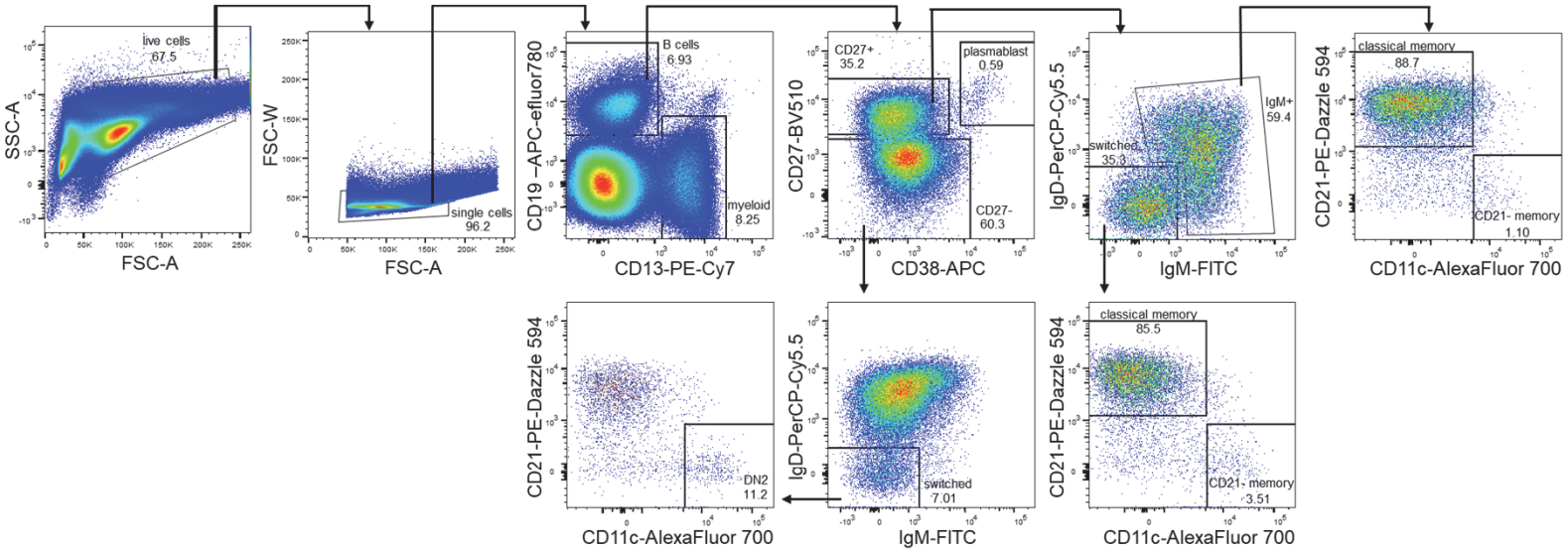


**b**

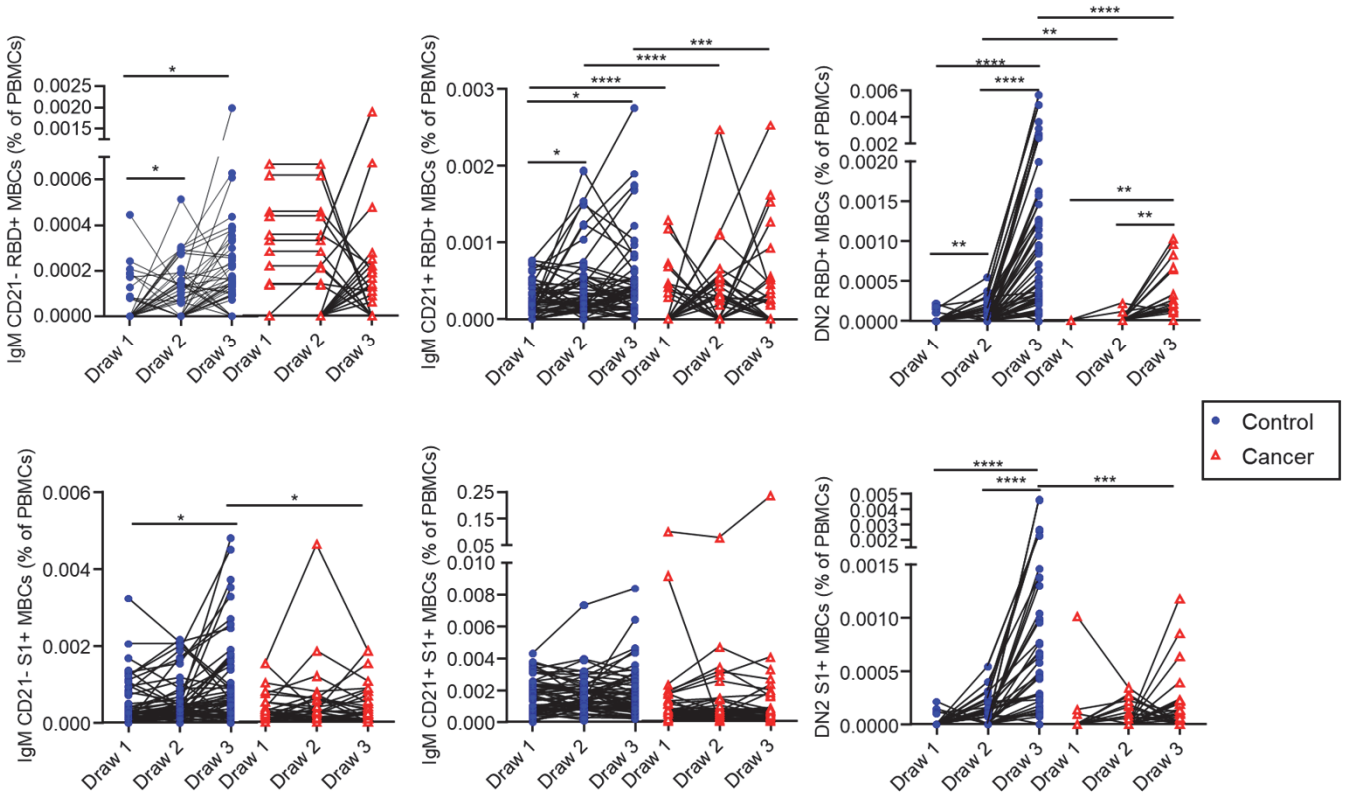

**Supplemental Figure 3: a,** Full gating strategy of memory B cell subsets (antigen-specific stains are shown in **Figure 4a**). **b,** Quantification of memory B cell subsets after vaccination. IgM or DN2 memory B cells are shown in plots. Cells that bind both RBD and S1 are annotated as RBD+, whereas cells that are specific only for S1 are denoted as S1+. Lines connect the same individual across blood draws, analyses were done on the arcsin of the square-root transformation, to standardize the small percentages. There is a statistically significant difference in slopes between cancer and control cohorts for RBD+ and S1+ ($p < 0.0001$ and $< 0.0001$, respectively) and the average rate of change is increasing in the control cohort for both RBD+ and S1+, though the magnitude is only statistically significant between draw 2 and 3 for RBD+ between the cancer cohort and the control cohort ($p=0.5806$ and $p< 0.0001$, respectfully) and S1+ ($p = 0.3511$ and $< 0.0001$, respectively) P-values were calculated by repeated measures ANOVA. *$p<0.05$; **$p<0.01$; ***$p<0.001$; ****$p<0.0001$